

Article

## The Impact of Selected Parameters on Visibility: First Results from a Long-Term Campaign in Warsaw, Poland

Grzegorz Majewski <sup>1,\*</sup>, Wioletta Rogula-Kozłowska <sup>2</sup>, Piotr O. Czechowski <sup>3</sup>, Artur Badyda <sup>4</sup> and Andrzej Brandyk <sup>5</sup>

<sup>1</sup> Division of Meteorology and Climatology, Faculty of Civil and Environmental Engineering, Warsaw University of Life Sciences, 166 Nowoursynowska St., 02-776 Warszawa, Poland; E-Mail: grzegorz\_majewski@sggw.pl

<sup>2</sup> Institute of Environmental Engineering, Polish Academy of Sciences, 34 M. Skłodowska-Curie St., 41-819 Zabrze, Poland; E-Mail: wioletta@ipis.zabrze.pl

<sup>3</sup> Gdynia Maritime University, Information Systems Department, 83, Morska St., 81-225 Gdynia, Poland; E-Mail: oskar@am.gdynia.pl

<sup>4</sup> Warsaw University of Technology, Faculty of Environmental Engineering, 20 Nowowiejska St., 00-653 Warszawa, Poland; E-Mail: artur.badyda@is.pw.edu.pl

<sup>5</sup> Water Centre Laboratory, Faculty of Civil and Environmental Engineering, Warsaw University of Life Sciences, 166 Nowoursynowska St., 02-776 Warszawa, Poland; E-Mail: andrzej\_brandyk@sggw.pl

\* Author to whom correspondence should be addressed; E-Mail: grzegorz\_majewski@sggw.pl.

Academic Editor: Armin Sorooshian

Received: 12 June 2015 / Accepted: 6 August 2015 / Published: 12 August 2015

---

**Abstract:** The aim of this study was to investigate how atmospheric air pollutants and meteorological conditions affected atmospheric visibility in the largest Polish agglomeration. The correlation analysis, principal component analysis (PCA) and generalized regression models (GRMs) were used to accomplish this objective. The meteorological parameters (temperature, relative humidity, precipitation, wind speed and insolation) and concentrations of the air pollutants (PM<sub>10</sub>, SO<sub>2</sub>, NO<sub>2</sub>, CO and O<sub>3</sub>) were recorded in 2004–2013. The data came from the Ursynów-SGGW, MzWarszUrsynów and Okęcie monitoring stations, located in the south of Warsaw (Poland). It was shown that the PM<sub>10</sub> concentration was the most important parameter affecting the visibility in Warsaw. The concentration, and indirectly the visibility, was mainly affected by the pollutant emission from the flat/building heating (combustion of various fuels). It changed intensively during the

research period. There were also periods in which this emission type did not have a great influence on the pollutant concentrations (mainly PM<sub>10</sub>) and visibility. In such seasons, the research revealed the influence of the traffic emission and secondary aerosol formation processes on the visibility.

**Keywords:** visibility; air pollutants; meteorological parameters; principal component analysis; generalized regression model

---

## 1. Introduction

The visibility deterioration caused by atmospheric pollution is a global problem. It occurs in many densely populated areas that have experienced population growth and industrialization. However, visibility is a complex issue. On one hand, it is directly affected by the anthropogenic air pollution. On the other hand, it is influenced by the meteorological conditions [1].

The anthropogenic air pollution effect on human health and visibility has been examined for decades. Many studies were conducted not only to assess the benefits for human health resulting from air pollutant emission reduction but also to understand how air pollutants negatively affect visibility. Generally, visibility makes a good index for the air pollution extent. It can also be used as a surrogate for assessing the human health effects [2,3].

The visibility impairment is mainly attributed to the scattering and absorption of the visible light caused by suspended particles and gaseous pollutants in the atmosphere [4,5]. The visibility impairment in the urban atmosphere is closely related to the air pollution from anthropogenic sources, such as car exhaust fumes, fuel combustion, solid waste incineration, and industrial emissions [6–10].

The visibility impairment is mainly influenced by the airborne particulate matter (PM), particularly its fine particles with aerodynamic diameters smaller than 2.5 µm (PM<sub>2.5</sub>). In urban areas, the major PM<sub>2.5</sub> components, such as ammonium, sulphates, nitrates, organic matter and elemental carbon [11], are the main factors contributing to the light absorption and scattering. Therefore, their presence effectively reduces visibility [12,13]. The specific content of PM<sub>2.5</sub> is the most important aspect when analysing the PM<sub>2.5</sub> effect on visibility. The size and chemical composition of each component particle affects its ability to refract, scatter, and absorb light [14]. There is a strong correlation between the presence of PM<sub>2.5</sub> and PM<sub>10</sub> (particles with aerodynamic diameters smaller than 10 µm), to the extent that a targeted reduction in PM<sub>10</sub> is likely to lead to an increase in the atmospheric visibility [15,16]. In addition to the air pollutants, the meteorological parameters (*i.e.*, wind speed and direction, relative air humidity, air temperature, atmospheric pressure and precipitation) can also directly or indirectly affect atmospheric visibility as they influence the local and regional air quality in urban areas [17–22].

Air quality monitoring has already been performed in Warsaw for about 20 years. Nevertheless, the measurement standards were adjusted to comply with the European Union (EU) regulations and requirements in 2004. Since then, the air quality has been successfully recorded in order to warn the community of high pollutant levels. The system also contributes to the research on air pollutant influence on human health [23,24]. The collected data also enables investigations into the air pollution impact on visibility. Taking into consideration the necessity to improve the visibility in urban areas,

the underlying mechanisms must be well understood, particularly when it comes to aspects such as the main contributing air pollutants and their origin. This research field has a worldwide significance. Nonetheless, it needs further development in Poland. Among the key statistical methods applied in this study, the researchers found the correlation analysis and the related Principal Component Analysis (PCA) and Generalized Regression Models (GRMs) particularly useful. All the models served to identify the air pollutants and meteorological parameters influencing visibility in an urban area.

## 2. Materials and Methods

### 2.1. Research Area

Warsaw is the biggest city in Poland and the ninth biggest city in Europe (517.24 km<sup>2</sup>). It is under the influence of the warm transitional temperate climate. The mean yearly air temperature is 8.6 °C. The mean precipitation sum is 550–650 mm. In Warsaw, the visible influence of a large urban agglomeration on the climate is seen as the so-called *urban heat island* [25]. The mean air temperatures and precipitation sums are higher whereas the wind speed is lower in the city center. As the air in the city is highly polluted, the cloud cover is bigger and the air transparency deteriorates. Consequently, the direct solar radiation decreases, whereas the diffuse sky radiation increases.

Even though the air quality has improved tremendously in Poland over the last 30 years [26–28], it is still unsatisfactory in Warsaw. What is definitely positive is the fact that the air pollutant levels (especially CO and SO<sub>2</sub>) have been gradually lowered over the last few years. Nonetheless, the permissible levels of PM<sub>10</sub> are still exceeded in the capital of Poland [29,30]. PM comes from many sources there, including, among others, the energy production sector and vehicular transport. The area of Warsaw is additionally threatened by the air inflowing from heavily polluted southern Poland [31]. PM composition in large urban areas of Poland differs significantly from the compositions observed in other urban areas in Europe [32–34]. There are higher contents of elemental (soot) and organic carbon and lower percentage of the secondary inorganic matter in PM. It seems that the differences must have a considerable impact on the visibility in the research area.

### 2.2. Air Quality Data and Visibility Observation

The study was based on the measurement results obtained from the MzWarszUrsynów monitoring station of the atmospheric air quality ( $\lambda_E = 21^\circ 02'$ ;  $\varphi_N = 52^\circ 09'$ ), located in the south of Warsaw (Figure 1). The researchers used the data on the mean hourly concentrations of the following air pollutants, measured by proper type of analyzers: sulphur dioxide (SO<sub>2</sub>)—MLU 100A, carbon monoxide (CO)—MLU 300, ozone (O<sub>3</sub>)—MLU 400, nitrogen oxides (NO<sub>2</sub>)—MLU 200A, and PM<sub>10</sub>—TEOM1400a. They were monitored with pulsed fluorescence, infrared absorption, ultraviolet light absorption, chemiluminescence, and a  $\beta$ -gauge automated particle sampler, respectively. The meteorological data came from the Ursynów-SGGW meteorological station ( $\lambda_E 21^\circ 02'$ ;  $\varphi_N 52^\circ 09'$ ). The following information was investigated: mean hourly air temperature values (T), insolation intensity (Rad), relative air humidity (RH), precipitation intensity (P) and wind speed (Ws). The measurements taken at the station were performed according to the instruction for network of stations belonging to the Institute of Meteorology and Water Management (IMGW). The data on the

visibility were obtained from the only station taking such measurements, *i.e.*, the Okęcie station ( $\lambda_E$  20°59';  $\varphi_N$  52°09'). The distance between the stations was approximately 6 km. The visibility measurements were carried out with a visibility meter equipped with an atmospheric phenomenon detector—Vaisala FS11 (wavelength 875 nm). It performed the functions of a visibility meter using light dispersion measurements and an atmospheric phenomenon detector. The horizontal visibility measurements were performed in the range of 10 m–50 km. The data (1-h values) were shared by the IMGW. The information used in the study came from 2004–2013. For the whole research period, the following numbers of data ( $n$ ) were obtained: visibility  $n = 87,634$ ; SO<sub>2</sub>,  $n = 85,416$ ; PM<sub>10</sub>  $n = 83,016$ ; NO<sub>2</sub>  $n = 85,985$ ; O<sub>3</sub>  $n = 85,148$ ; T  $n = 85,936$ ; RH  $n = 86,205$ ; Rad  $n = 85,384$ .

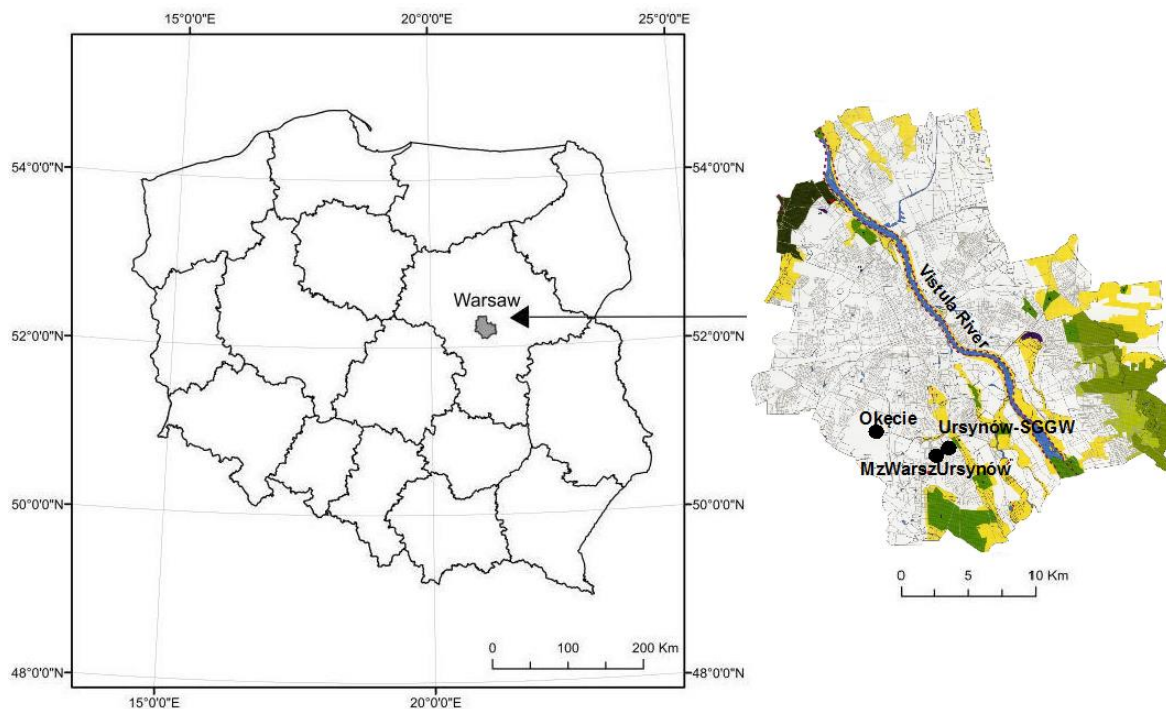


**Figure 1.** Location of the measurement stations in Warsaw (Poland).

### 2.3. Statistical Method

The correlation analysis, principal component analysis (PCA) and generalized regression models (GRMs) were applied in this research. The analyses helped to identify factors affecting visibility.

Generally, the PCA is a data reduction exercise. It is achieved through finding linear combinations (principal components) of the original variables, which account for as much of the original total variance as possible [16,17,19,35,36]. PCA is used to identify factors and their synergies in strong measurements scales: interval and ratio. Here, a scale or a level of measurement is the classification that describes the nature of information within the numbers assigned to variables. The interval type allows for the degree of difference between items, but not the ratio between them. The ratio type takes its name from the fact that measurement is the estimation of the ratio between a magnitude of a continuous quantity and a unit magnitude of the same kind.

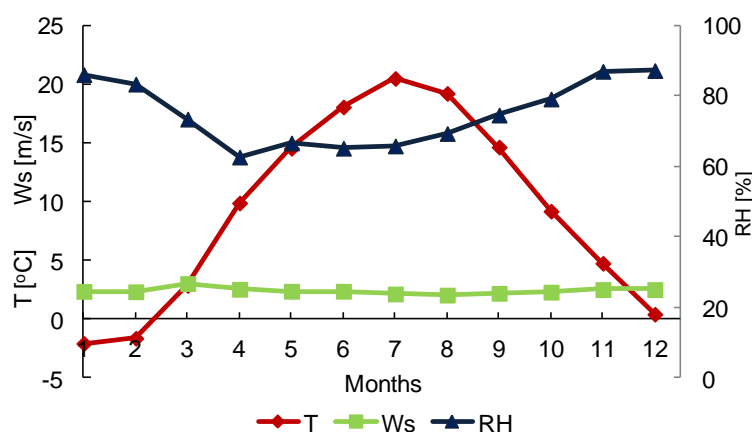
GRM's models were used to identify factors in weak measurements scales: nominal and ordinal (ex. seasonality), and additionally, jointly with variables in strong scales. Nominal scales refer to the

construction of classification of items, while ordinal ones allow for rank order by which data can be sorted. GRM is considered to be a path, embracing more than a model. It enabled to find the “best” model, describing the analysed phenomenon, out of an available range of models, and to replace many classical ones (e.g., ANOVA, MANOVA). Such an approach is more efficient for replication and cross-validation studies, less costly to put into practice in predicting and controlling the outcome in the future. Finally, it allows use of a wider range of fit statistics and diagnostic calculations, than using single models separately [21,37,38].

### 3. Results and Discussion

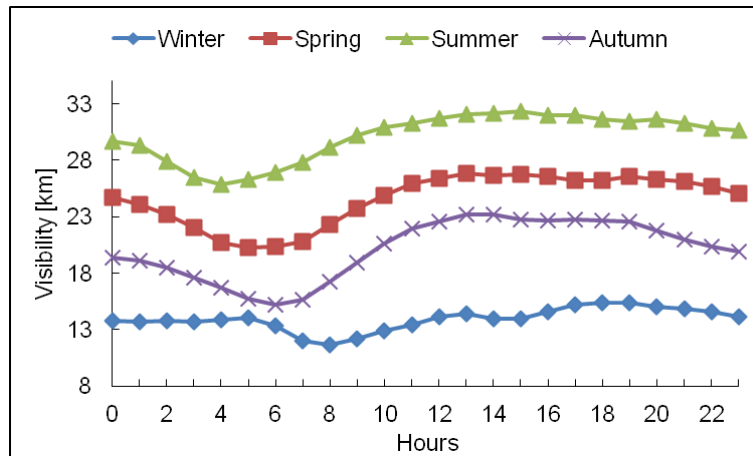
#### 3.1. General Description of Visibility, Meteorology and Air Pollution

The yearly course of the air temperature (average in the period 2004–2013) was typical for the temperate and transitional climate in Poland. July was the warmest month (mean air temperature = 20.5 °C). January was the coldest month (mean air temperature = −2.1 °C). The lowest wind speed values were measured in August and September (approx. 2.1 m/s), whereas the highest ones were observed in March (3.1 m/s)—Figure 2.



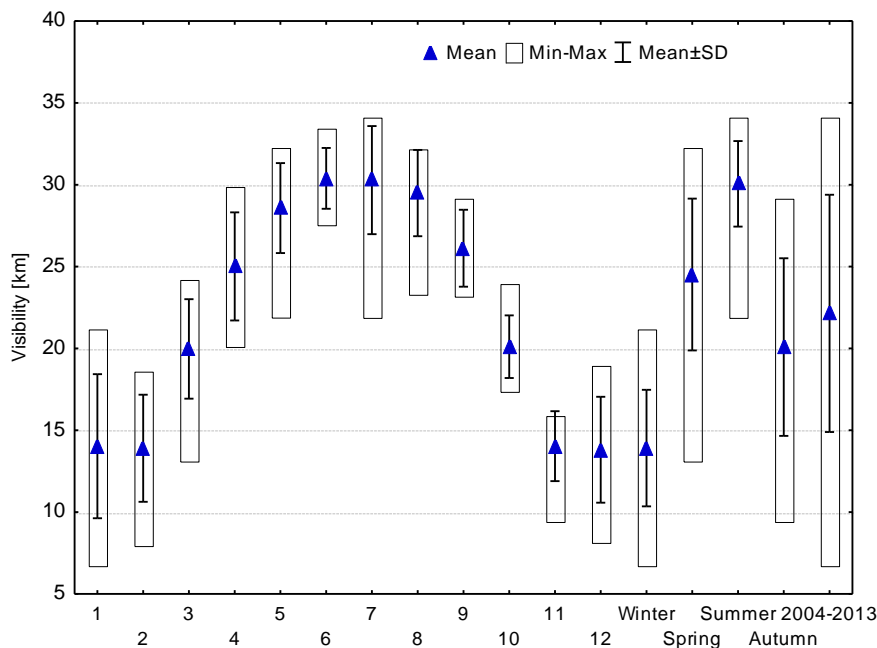
**Figure 2.** Monthly variations of meteorological parameters over Warsaw in 2004–2013.

Figure 3 presents the diurnal patterns of visibility for the period 2004–2013. Visibility shows an obvious diurnal variation in each season of the year. In spring (March, April, May) and summer (June, July, August), a valley appears in early morning, from 04:00 to 06:00, while in autumn (September, October, November) and spring it is observed slightly later, between 06:00 and 07:00. The peak appears generally in the afternoon, from 13:00 to 15:00, except for winter (December, January, February), for which the peak is slightly later, at about 18:00. Visibility shows stronger diurnal cycles in summer and autumn, while it exhibits a much weaker variation in winter. Apart from this, the diurnal patterns during different seasons are desynchronized, which is attributed to the difference in weather patterns and stability of atmospheric boundary layer. The diurnal variation of visibility, characteristic for the city of Warsaw, is similar to that over several cities in China, however, hourly visibility values are found to be three times higher than those recorded in the Chinese cities [19].



**Figure 3.** Diurnal variations of visibility over Warsaw for winter (December, January, February), spring (March, April, May), summer (June, July, August) and autumn (September, October, November) in 2004–2013.

For the whole research period (2004–2013) monthly visibility was in a wide range of 6.7–34.1 km (Figure 4). Within the researched period, noticeable seasonal changes in visibility were found. Visibility was generally higher in summer and lower in late autumn and winter. The average seasonal visibilities were 24.5, 30.1, 20.1, and 13.9 km in spring, summer, autumn, and winter, respectively (Figure 4).



**Figure 4.** Descriptive statistics of monthly and seasonal visibility over Warsaw in 2004–2013.

Monthly visibility in Warsaw exhibited, in general, a considerable winter period variation (January–March, October–November) from 2004–2013. The summer period was characterized by much lower variation.

The mean yearly visibilities were in the range of 19.8–23.7 km (Figure 5). This proves that it did not show significant variability year by year. However, monthly values exhibit an increasing trend

throughout the research period, but are statistically insignificant;  $p < 0.05$  (Figure 6). Average visibility for the whole period 2004–2013 was equal to 22.1 km and is from 5.3 km to over 13.1 km higher than the one over large, highly-urbanized cities of China [1,19].

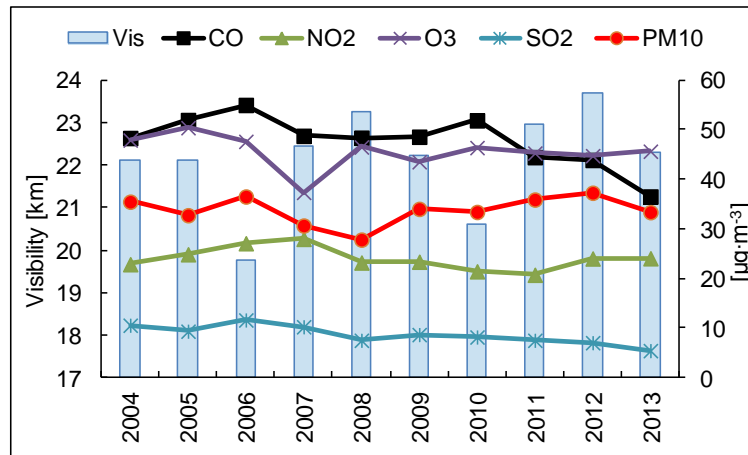


**Figure 5.** Yearly variations of visibility and ambient concentrations of NO<sub>2</sub>, O<sub>3</sub>, SO<sub>2</sub>, PM<sub>10</sub> and CO (divided by 10 in the figure) over Warsaw in 2004–2013.

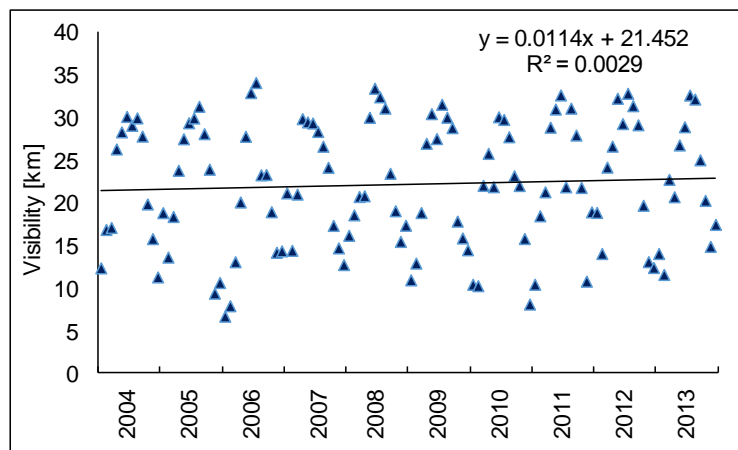


**Figure 6.** Visibility time series of monthly mean and its’ linear regression trend over Warsaw in 2004–2013.

From 2004–2013 yearly air pollutants concentration didn’t show much variation, alike visibility. In the analysed years, the mean yearly concentrations of NO<sub>2</sub> were 21.4–28.0 µg·m<sup>-3</sup>, which made 53.6%–70% of the permissible value (40 µg·m<sup>-3</sup>)—Figure 5. The mean yearly concentrations of SO<sub>2</sub> were 5.5–11.5 µg·m<sup>-3</sup> (the permissible value; 20 µg·m<sup>-3</sup>), and the mean yearly concentrations of CO were 365.7–549.5 µg·m<sup>-3</sup>. The mean yearly concentrations of PM<sub>10</sub> did not exceed the permissible value as well (40 µg·m<sup>-3</sup>) and were in the range of 28.0–37.2 µg·m<sup>-3</sup>. The only pollutant, that, according to the Polish applicable laws, exceeded the permissible limit, was the ozone O<sub>3</sub>. The mean yearly concentrations of O<sub>3</sub> were 43.5–50.4 µg·m<sup>-3</sup>. The permissible level of the 8-h O<sub>3</sub> concentration is 120 µg·m<sup>-3</sup> and can be exceeded about 25 days in each year. The biggest number of days with the exceeded value was observed in 2005. In the research area, there was no steady trend in the changes for O<sub>3</sub>, which is a secondary pollutant. The changes in its concentration mainly resulted from the

changes in the weather conditions (insolation intensity, air temperature) and the participation of the O<sub>3</sub> precursors (e.g., nitrogen oxides, hydrocarbons and other pollutants participation in the O<sub>3</sub> formation) in the atmospheric air [30,39].

Since the visibility is strongly affected by air pollutants [1,40,41], the presence of its' weaker variation over Warsaw from 2004–2013 is found. In Poland, considerable changes in air pollution were observed from 1980–2000 [42]. In that period, political and economical transformation was related with a sudden decrease of industrial emission due to large factories closure and limited production in remaining ones [43,44]. On the other hand, such transformation contributed to the knowledge on negative consequences of air pollution, and for this reason in 1980s industrial emissions were largely restricted in Poland. Unfortunately, no reliable air pollution measurements were then performed within the research area.

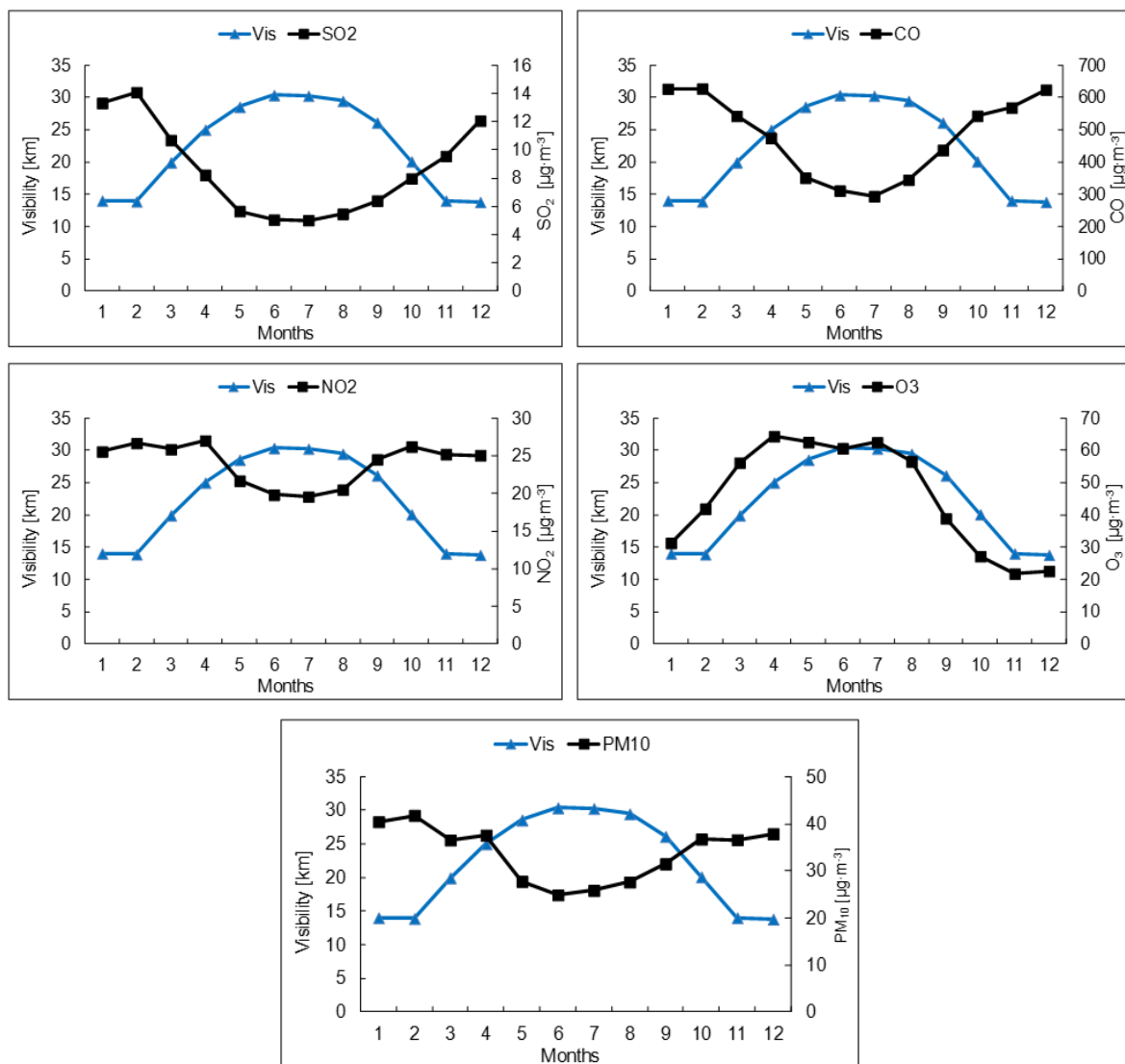


**Figure 7.** Monthly variations of visibility and ambient concentrations of air pollutants over Warsaw in 2004–2013.

Monthly visibilities and monthly ambient concentrations of air pollutants (averages for the whole period 2004–2013) are shown in Figure 7. Comparing the maximum and minimum values for the

monthly concentrations shows that O<sub>3</sub>, CO and SO<sub>2</sub> have the largest variability; while much lower variability was shown by PM<sub>10</sub> and NO<sub>2</sub>. Visibility values were inversely proportional to all analysed pollutants, except for O<sub>3</sub>. Ambient concentrations of PM<sub>10</sub>, SO<sub>2</sub>, NO<sub>2</sub> and CO tend to be strongly affected by the emission from fuel combustion for heating purposes [31,45]. It is obvious that their concentration is higher in winter months, while the visibility becomes lower (Figure 7). Except for the higher winter emission in Poland, the increase of air pollution is also attributed to meteorological conditions (lowering of air mixing layer, stagnant air) that deteriorate ventilation and ability of self-cleaning [46]. The fact that concentrations of CO, NO<sub>2</sub> and SO<sub>2</sub> are higher in the cold season (Figure 7) is attributed to increased emissions—however, the atmospheric lifetime of these compounds is also generally longer in the winter and this is likely to explain some of the increase as well.

The mean NO<sub>2</sub> concentration was slightly higher in the cold season than in the warm one. Such a situation was related to the low variation of the yearly NO<sub>2</sub> emission. Typically, the data indicated two daily peaks in the ambient concentrations of both NO<sub>x</sub> forms (NO and NO<sub>2</sub>), which pointed to the traffic-related pollution [30,39]. Emission from the traffic contributes also to ambient concentrations of volatile organic compounds (VOCs). VOCs and NO react with O<sub>3</sub> giving a loss of O<sub>3</sub> near to pollution sources. On the other hand, higher O<sub>3</sub> in summer is probably because of higher solar insolation, and visibility is lower because of the lack of cold season emissions and boundary layer effects. For those reasons, the course of monthly ozone concentrations is different from NO<sub>2</sub> and other pollutants, and resembles the course of visibility.

### 3.2. Visibility during Periods Differing in the Air Pollution with PM

Table 1 presents the mean values of visibility, PM<sub>10</sub>, gaseous pollutants and meteorological parameters (calculated on the basis of 1-h values from the entire research period) grouped within three categories: clear days (PM<sub>10</sub> concentration did not exceed 50 µg·m<sup>-3</sup>), moderate days (PM<sub>10</sub> concentration was 50–200 µg·m<sup>-3</sup>) and episode days (PM<sub>10</sub> concentration exceeded 200 µg·m<sup>-3</sup>).

The NO<sub>2</sub> concentration was 3.7 times higher during the episodes than on the clear days (20.4 µg·m<sup>-3</sup>), while the CO concentration was approximately six times higher. A similar situation was observed for SO<sub>2</sub>. For O<sub>3</sub>, an inverse correlation was observed. Its lowest concentrations were found for the episode days. The episodes were characterized by low mean visibility (6.0 km), low air temperature, low wind speed, and higher relative air humidity. On the other hand, the clear days were characterized by the highest mean visibilities (24.3 km), higher wind speeds and lower relative air humidity. Episode days occurred mostly in winter, while clear days were found in warm periods, mostly in summer. Unfortunately, the researchers did not have data on the mixed layer height and atmospheric pressure. As different studies show, high atmospheric pressure leads to the lower mixed layer height and low wind speed, which causes increased pollutant concentrations close to the pollutant sources and visibility deterioration. Low atmospheric pressure results in the higher mixed layer height and high wind speed, which provides effective ventilation for cities and good dispersion of pollutants [6]. The research conducted by Majewski *et al.* [29] into the atmospheric pressure influence on the PM<sub>10</sub> concentration in Warsaw showed that the increase in the PM concentration was significantly statistically related to the increase in the atmospheric pressure.

**Table 1.** Values of visibility and other parameters calculated as arithmetic means on the basis of the hourly values from 2004–2013 for three periods differing in the air pollution with PM.

Parameter	Air Quality		
	PM <sub>10</sub> < 50 <sup>a</sup> µg·m <sup>-3</sup> Clear Days	PM <sub>10</sub> > 50 <sup>a</sup> µg·m <sup>-3</sup> Moderate Days	PM <sub>10</sub> > 200 <sup>b</sup> µg·m <sup>-3</sup> Episode
Occurrence number (hours)	68,652	14,285	146
PM <sub>10</sub> (µg·m <sup>-3</sup> )	25.7	75.1	236.1
SO <sub>2</sub> (µg·m <sup>-3</sup> )	6.8	12.6	28.1
CO (µg·m <sup>-3</sup> )	378.8	822.1	2342.4
NO <sub>2</sub> (µg·m <sup>-3</sup> )	20.4	40.5	76.0
O <sub>3</sub> (µg·m <sup>-3</sup> )	48.5	28.9	14.0
Visibility (km)	24.3	13.6	6.0
Temperature (°C)	10.5	4.7	-6.9
Wind speed (m·s <sup>-1</sup> )	2.7	1.7	1.1
Relative humidity (%)	73.4	77.7	78.9

<sup>a</sup> Permissible level for the 24-h PM<sub>10</sub> concentration due to the human health protection in Poland. <sup>b</sup> Threshold value for informing the inhabitants about the risk of exceeding the alert level for PM<sub>10</sub> in Poland.

### 3.3. Weekend/Weekday Differences in Visibility and Air Pollution

When referring to the visibility and air quality studies, there is a phenomenon known as the *weekend effect*. Studies on this phenomenon can help to better understand the emission characteristics of air pollutants in urban areas and the weekend effect has been reported in America since the 1970s [47,48]. Contemporary research is especially focusing on visibility variations and the effect of air quality on visibility on weekdays compared with weekend days. In order to investigate potential weekend effect over Warsaw, mean weekend and weekday levels of visibility as well as air pollutants were calculated and subjected to Fisher–Snedecore test. Visibilities on weekends were slightly better than on weekdays, and the differences were statistically significant. Mean hourly visibility was equal to  $22.61 \pm 12.57$  km at weekends and slightly over  $22.02 \pm 12.71$  on weekdays (Table 2). For PM<sub>10</sub>, slightly higher and statistically significant weekday concentrations were observed, as well as for SO<sub>2</sub>, which was slightly lower during weekends. We also found CO concentrations to become lower on weekends (statistically significant differences) and, moreover, mean weekend and weekday NO<sub>2</sub> concentrations over Warsaw showed statistically significant differences, with NO<sub>2</sub> concentration higher on weekdays. This is probably due to less vehicular emission on weekends.

All concentrations of airborne pollutants were higher during weekdays, (statistically significant differences), except ozone. O<sub>3</sub> concentration was higher at weekends even though the O<sub>3</sub> pollutant precursor concentrations (such as NO<sub>x</sub> and volatile organic compounds) are lower on weekends [47,48]. The weekend effect in the O<sub>3</sub> concentrations is the most likely to be attributable to decreased O<sub>3</sub> destruction by NO<sub>x</sub>, as there are lower emissions from its' main source—communication and vehicular transportation [48,49]. The result of this study, concerning lower concentrations of airborne pollutants on weekends, excluding ozone, is similar to that obtained by Tsai [17].

**Table 2.** Visibility and air pollutant concentrations calculated as arithmetic means on the basis of the hourly values from 2004–2013 for two different periods—weekends and week days.

	Vis	PM <sub>10</sub> (µg·m <sup>-3</sup> )	SO <sub>2</sub> (µg·m <sup>-3</sup> )	CO (µg·m <sup>-3</sup> )	NO <sub>2</sub> (µg·m <sup>-3</sup> )	O <sub>3</sub> (µg·m <sup>-3</sup> )
Weekend	22.61 ± 12.57 (n = 25,044)	32.03 ± 24.20 (n = 23,652)	8.08 ± 6.95 (n = 24,485)	456.45 ± 327.25 (n = 23,782)	20.20 ± 15.74 (n = 24,585)	48.94 ± 29.46 (n = 24,444)
Weekday	22.02 ± 12.71 (n = 62,590)	34.66 ± 25.38 (n = 59,364)	8.75 ± 8.15 (n = 60,931)	485.49 ± 340.51 (n = 59,495)	25.50 ± 17.60 (n = 61,400)	44.51 ± 29.94 (n = 60,704)
Fisher test	62,590	59,364	60,931	59,495	61,400	60,704
p-value	0.0000	0.0000	0.0000	0.0000	0.0000	0.0000

### 3.4. Correlations between Pollutants, Meteorological Variables and Visibility

Total correlations found between the results of the visibility measurements and other measurements (mean hourly values) in the whole research period are shown in Table 3. The visibility measurement results were negatively correlated with CO, PM<sub>10</sub>, SO<sub>2</sub> and NO<sub>2</sub>. Therefore, the increase in CO and SO<sub>2</sub> concentrations corresponds with visibility decrease, and PM<sub>10</sub> and NO<sub>2</sub> are those species, that can directly contribute to visual range limitations.

**Table 3.** Correlation matrix for total parameters measured for the entire period of 2004–2013 (correlations calculated for hourly values) and arithmetic means and standard deviations of the hourly value sets for the measured parameters.

	A	SD	PM <sub>10</sub>	SO <sub>2</sub>	CO	NO <sub>2</sub>	O <sub>3</sub>	T	Ws	RH	Rad	P
Vis (km)	22.19	12.67	-0.33	-0.27	-0.37	-0.21	0.47	0.52	0.14	-0.60	0.37	-0.10
PM <sub>10</sub> (µg·m <sup>-3</sup> )	33.91	25.07	1.00	0.37	0.66	0.56	-0.26	-0.23	-0.25	0.05	-0.13	-0.04
SO <sub>2</sub> (µg·m <sup>-3</sup> )	8.56	7.83		1.00	0.34	0.25	-0.15	-0.38	-0.10	0.10	-0.07	-0.03
CO (µg·m <sup>-3</sup> )	477.20	337.03			1.00	0.62	-0.41	-0.38	-0.28	0.21	-0.25	-0.03
NO <sub>2</sub> (µg·m <sup>-3</sup> )	23.98	17.26				1.00	-0.52	-0.19	-0.36	0.15	-0.31	-0.03
O <sub>3</sub> (µg·m <sup>-3</sup> )	45.78	29.87					1.00	0.47	0.22	-0.71	0.56	0.02
T (°C)	9.33	9.33						1.00	0.03	-0.52	0.48	0.05
Ws (m/s)	2.42	1.68							1.00	-0.08	0.16	0.04
RH (%)	74.97	18.82								1.00	-0.58	0.06
Rad (W/m <sup>2</sup> )	117.77	200.98									1.00	-0.03
P (mm)	0.07	0.52										1.00

Notes: A: mean value; SD: standard deviation; Vis: visibility; T: temperature; RH: relative air humidity; Ws: wind speed; Rad: insolation intensity; P: precipitation.

Visibility was positively correlated with the O<sub>3</sub> concentrations. The atmospheric O<sub>3</sub> is a secondary air pollutant formed in photochemical reactions. Hence, summer is the period of the most intense O<sub>3</sub> formation. It resulted from the high insolation intensity during this season. The observed correlation was caused by the fact that both parameters (visibility and O<sub>3</sub> concentrations) increased and decreased in the same periods (Figure 7).

In addition to their impact on visibility via changing the concentration of pollutants, meteorological variables can affect the visibility more directly - as humidity increases, hygroscopic aerosols increase

in size and thus the scattering of light by them increases. At some point, aerosols activate and become fog [50,51]. This transition is very complex and has a very large impact on visibility [50,51].

Hourly visibility exhibited low, negative correlation with precipitation (Table 3). Generally, the precipitation lowered the air pollutant concentrations through the precipitation scavenging. Thereby, visibility increased [52]. However, the air purification effect and related visibility improvement appears with a delay after rainy days. During heavy precipitation visibility will be reduced. However, after the precipitation has stopped, the aerosols concentration are likely to be lower, thus giving two opposite impacts with a visibility increase following rain. In fact, the visibility reduction is more likely caused by the scattering of light by the hydrometeors. There is a negative correlation between precipitation and the primary pollutants, but this is weak and may relate to improved boundary layer ventilation when there is precipitation rather than scavenging. This is suggested by the fact that the relatively insoluble CO and NO<sub>2</sub> have a negative correlation with precipitation, which is the same size as that of the more soluble SO<sub>2</sub>.

Visibility was positively correlated with the three remaining meteorological parameters, air temperature, insolation intensity, and wind speed. Most likely under clear sky conditions, the temperatures increase, the relative humidity falls and so the aerosols shrink, thus increasing the visibility.

### 3.5. Principal Component Analysis (PCA)

PCA served to extract four principal components (new variables: PC1, PC2, PC3 and PC4) with eigenvalues >1.0, which accounted for 73% of the total variance (Table 4). PC1, PC2, PC3 and PC4 can be interpreted as major factors that control visibility [1,6,17,40]. Visibility (Vis), O<sub>3</sub> concentration (O<sub>3</sub>), NO<sub>2</sub> concentration (NO<sub>2</sub>), CO concentration (CO), air temperature (T), relative air humidity (RH), PM<sub>10</sub> concentration (PM<sub>10</sub>) and insolation intensity (Rad) were most strongly correlated with PC1. Knowing the research area and the influence of various emission sources in this region, it can be assumed that PC1 could be related to fuel combustion for heating (mainly hard coal, wood/biomass and heating/crude oil) [31,44]. The emission increased over the year along with the T drop and Rad decrease. At the same time, the pollutant concentrations (*i.e.*, PM<sub>10</sub>, NO<sub>2</sub>, CO, or SO<sub>2</sub>) in the air increased. Simultaneously, the photochemical pollutant concentrations (represented by O<sub>3</sub>) decreased. Visibility was reduced in periods of high air pollution, related with heating (opposite signs for Vis/PC1 correlation and PM<sub>10</sub>, NO<sub>2</sub>, CO, SO<sub>2</sub>/PC1 correlation).

The PCA performed only for the cold season data (Table 5) confirmed the same correlations between PC1 and the air pollution with NO<sub>2</sub>, SO<sub>2</sub> and CO, and the inverse (opposite signs) correlation between PC1 and visibility, O<sub>3</sub> concentration, air temperature and insolation. For the warm season, the PCA revealed a very strong correlation between PC1 and NO<sub>2</sub> and an inverse strong correlation (opposite signs) between PC1 and visibility, O<sub>3</sub> concentration and insolation. Most likely, in those periods when there is less pollution from heating, and temperature rises, air pollution is mainly shaped by traffic emissions [31]. Then, the increase of NO<sub>2</sub> is observed, which reacts with O<sub>3</sub> and in consequence the concentration of O<sub>3</sub> in the air decreases. The reaction intensity becomes higher when the insolation intensity is stronger (O<sub>3</sub> concentrations and insolation were correlated with PC1 in the same way). Under such conditions, visibility may be improved (contrary signs of Vis/PC1 and NO<sub>2</sub>/PC1). Nonetheless, it is not possible to discuss the cause-and-effect correlation between the traffic emission (and the related

photochemical reactions) and the visibility increase or decrease. Most probably, visibility increased because the air pollution with PM was lower and the temperature and insolation were higher in summer.

**Table 4.** Correlations between the principal components (PC1, PC2, PC3, PC4) and measured parameter values. The PCA was performed for the hourly data collected in 2004–2013.

Component	PC1	PC2	PC3	PC4
Vis	<b>0.7</b>	0.3	0.2	0.2
PM <sub>10</sub>	<b>-0.6</b>	<b>0.6</b>	-0.1	-0.1
SO <sub>2</sub>	-0.4	0.3	<b>-0.6</b>	0.0
CO	<b>-0.7</b>	0.5	0.0	-0.1
NO <sub>2</sub>	<b>-0.7</b>	0.5	0.3	0.0
O <sub>3</sub>	<b>0.8</b>	0.3	-0.3	-0.1
T	<b>0.7</b>	0.3	0.4	-0.2
Ws	0.4	-0.3	-0.5	0.0
RH	<b>-0.7</b>	<b>-0.6</b>	0.1	0.0
Rad	<b>0.6</b>	0.4	-0.3	-0.1
P	0.0	-0.2	0.0	<b>-0.9</b>
eigenvalue	4.06	1.79	1.12	1.02
% total variance	37	16	10	9
Cumul. % variance	37	53	63	73

**Table 5.** Correlations between the principal components (PC1, PC2, PC3) and measured parameter values. The PCA was performed for the hourly data collected in 2004–2013, separately for the cold (January–March and October–December) and warm (April–September) seasons.

Component	Season	PC1	PC2	PC3	Season	PC1	PC2	PC3
Vis.		<b>-0.7</b>	0.3	-0.1		-0.5	-0.3	-0.5
PM <sub>10</sub>		<b>0.7</b>	0.5	-0.1		0.4	<b>-0.7</b>	0.2
SO <sub>2</sub>		0.4	0.4	0.4		0.1	-0.4	0.5
CO		<b>0.8</b>	0.4	-0.1		<b>0.6</b>	-0.5	0.1
NO <sub>2</sub>		<b>0.7</b>	0.3	-0.3		<b>0.7</b>	-0.5	-0.1
O <sub>3</sub>		<b>-0.7</b>	0.4	0.4		<b>-0.8</b>	-0.2	0.2
T	cold	-0.4	-0.1	<b>-0.8</b>	warm	<b>-0.6</b>	-0.4	0.0
Ws		<b>-0.6</b>	0.0	0.0		-0.4	0.3	0.4
RH		0.5	<b>-0.8</b>	0.1		<b>0.7</b>	<b>0.6</b>	0.0
Rad.		-0.4	<b>0.6</b>	-0.1		<b>-0.7</b>	-0.2	0.2
P		0.0	-0.3	0.0		0.0	0.2	<b>0.6</b>
Eigen value		3.59	1.84	1.12		3.46	1.99	1.14
% total variance		33	17	10		31%	18%	10%

PC2 was most strongly but differently (opposite signs) correlated with the PM<sub>10</sub> concentrations and relative air humidity (Table 4). Visibility, pollutant concentrations, temperature and insolation were correlated with PC2 in the same way as PM<sub>10</sub> but to a lesser extent. Thus, PC2 reflected the situation when the concentrations of all the observed pollutants and visibility decreased whereas the relative air

humidity and precipitation increased. While humidity increases, hygroscopic aerosols increase in size and thus the scattering of light by them increases, so visibility drops. Air humidity concentration in the air was high due to precipitation at high temperature. During precipitation, concentrations of all the pollutants decreased due to leaching. The situation concerned PM<sub>10</sub> to the largest extent.

3.6. Generalized Regression Model (GRM)

The GRM identification was performed to finally confirm the influence of the analysed factors on visibility. It concerned the observations of the measured parameters and other defined factors, such as the influence of a season or specific year or combination of these factors. It was assumed that a given factor would be introduced into the model, if the value *F* (*F*—Fischer-Snedecor distribution) characterizing the significance of the factor contribution into the dependable variable forecasting (visibility) was higher than *F*<sub>1</sub>. The factor was removed if its *F* was lower than *F*<sub>2</sub> (Table 6).

**Table 6.** Generalized Regression Model (GRM) summary: variables introduced into the model due to estimation.

Variable	Model Steps	Degrees of Freedom	<i>F</i> <sub>2</sub> for out	<i>p</i> <sub>2</sub> for out	<i>F</i> <sub>1</sub> for in	<i>P</i> <sub>1</sub> for in	Effect
RH	16	1	1594.25	0.00000			In model
lnPM <sub>10</sub>		1	389.95	0.00000			In model
Season		1	64.60	0.00000			In model
Precipitation Y N		1	233.19	0.00000			In model
O <sub>3</sub>		1	66.46	0.00000			In model
lnCO		1	92.79	0.00000			In model
T		1	24.39	0.00000			In model
Rad		1	41.06	0.00000			In model
Ws		1	36.40	0.00000			In model
YEAR		9	6.42	0.00000			In model
Year * Season		9	5.78	0.00000			In model
lnSO <sub>2</sub>		1	21.37	0.00000			In model
Year * Prec.Y N		9	3.68	0.00013			In model
Season * Prec.Y N		1	13.53	0.00023			In model
lnNO <sub>2</sub>		1	10.67	0.00109			In model
Year * Season * Prec.Y N		9			0.629	0.773	Out of model

Before the identification, the variables underwent necessary analyses and transformations. The variables that were at least in the interval scales were submitted to the quality assessment and logarithming (Box-Cox transformation with the Lambda parameter = 0.5). The precipitation variable was taken to the nominal scale, where 0 and 1 meant the hours without and with precipitation, respectively (variable: Prec.Y|N).

Table 6 presents the results of the stepwise estimation for the GRM. The variables, seasonal factors and their interactions marked “in model” turned out to be significantly affecting visibility. Hence, they were introduced into the model. Table 7 presents the adjustment of the model that was finally selected

as the best one with consideration for the maximum adjustment criterion and minimum number of the independent variables.

**Table 7.** Assessment of the GRM adjustment.

	Multipl.—R	Multipl.—R <sup>2</sup>	Correct.—R <sup>2</sup>	SS—Model	df—Model	MS—Model	SS—Rest	Df—Rest	MS—Rest	F	p
Vis	0.75	0.56	0.56	6499948	39	166665.3	5033049	71764	70.133	2376.4	0.00

To picture the significance of the variables, they were ordered following the values of the Student’s *t*-distribution for the assessment of the model parameter significance (Figure 8—Pareto chart). The higher the *t*-value was, the more important the significance of the factor was for explaining its influence on visibility. Relative air humidity and PM<sub>10</sub> were two most important factors affecting visibility on the basis of the identified model. The influence exerted by SO<sub>2</sub> and NO<sub>2</sub> on visibility was much lower from the impact that other analysed pollutants had. The results also show the influence of the seasonality, atmospheric precipitation (its presence or lack; variable: Prec.Y|N) and interactions between the periods (e.g., season \* month) on visibility.

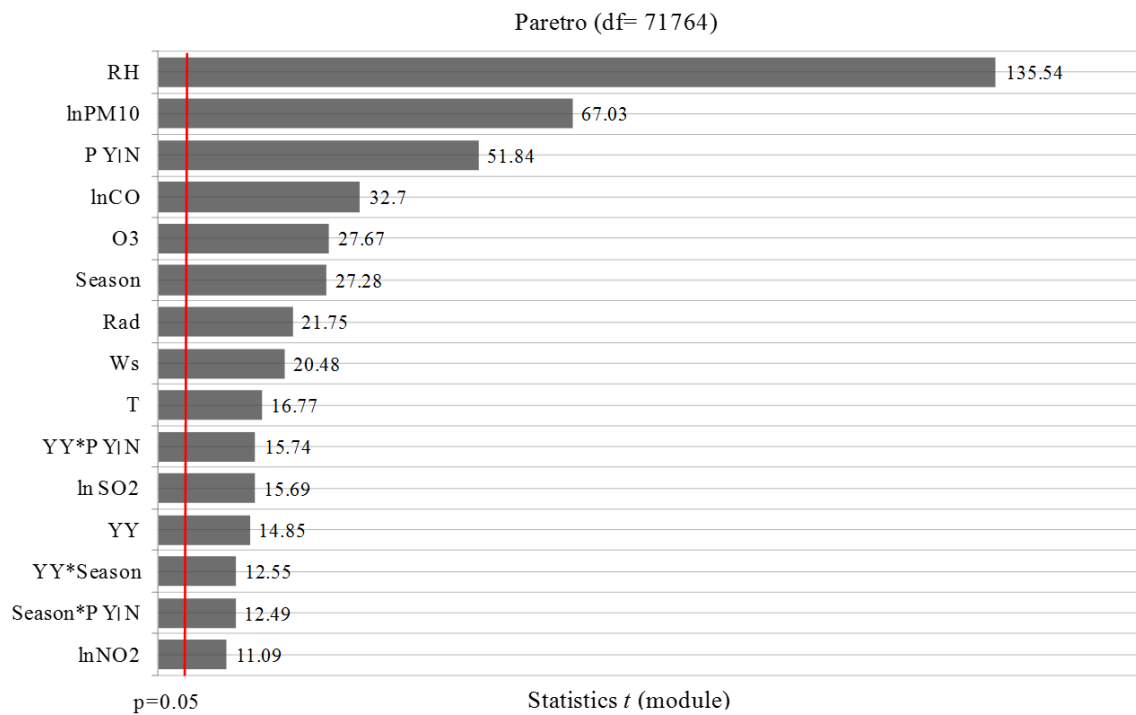


**Figure 8.** Pareto chart for the significance of factors affecting visibility in the GRM.

Table 8 presents estimated parameter values for the selected GRM (Tables 6 and 7), together with estimations for the parameter errors, *t*-distribution and p-value indicating the variable significance and coincidence with visibility. In a statistical sense, it was shown that the relative air humidity and wind speed variations corresponded with visibility more than the temperature. It was also revealed that visibility was most likely sensitive to the changes in the PM<sub>10</sub> and CO concentrations. Specifically, a 50% drop in the PM<sub>10</sub> concentration could be associated with visibility improvement by 2.9 km. On the other hand, a drop in the CO concentration by 50% corresponded with the visibility being increased by 2.2 km, however, there was no evidence for a direct cause-and-effect relationship. The

50% decrease in the O<sub>3</sub> concentration might only slightly affect the visibility increase, as suggested by the performed regression analyses.

**Table 8.** Estimated parameter values for the selected GRM with estimations of parameter errors, *t*-distribution and *p*-value indicating the variable significance.

Regression Coefficient	Level/Effect	Estimated Regression Coefficient	Estimated Standard Deviation	<i>t</i>	<i>p</i> Value
Intercept		82.615	0.633	130.468	0.000
lnSO <sub>2</sub>		-0.902	0.057	-15.692	0.000
lnNO <sub>2</sub>		0.827	0.075	11.089	0.000
lnCO		-3.122	0.095	-32.699	0.000
O <sub>3</sub>		-0.054	0.002	-27.673	0.000
T		0.097	0.006	16.766	0.000
Ws		0.450	0.022	20.479	0.000
RH		-0.395	0.003	-135.537	0.000
Rad		-0.005	0.000	-21.751	0.000
lnPM <sub>10</sub>		-4.220	0.063	-67.032	0.000
YY	2004	0.727	0.163	4.467	0.000
YY	2005	-0.736	0.164	-4.495	0.000
YY	2006	-1.829	0.168	-10.867	0.000
YY	2007	0.880	0.175	5.024	0.000
YY	2008	0.913	0.165	5.540	0.000
YY	2009	2.028	0.137	14.847	0.000
YY	2010	-1.619	0.162	-9.997	0.000
YY	2011	1.174	0.115	10.182	0.000
YY	2012	-0.287	0.142	-2.016	0.044
Season	warm	1.695	0.062	27.284	0.000
Prec. Y N	Non-raining	2.698	0.052	51.837	0.000
Year * Season	1	0.197	0.096	2.048	0.041
Year * Season	2	-0.857	0.095	-9.028	0.000
Year * Season	3	-1.132	0.093	-12.119	0.000
Year * Season	4	-0.189	0.104	-1.815	0.070
Year * Season	5	-1.052	0.105	-10.023	0.000
Year * Season	6	-0.276	0.092	-3.010	0.003
Year * Season	7	0.814	0.101	8.036	0.000
Year * Season	8	0.531	0.093	5.730	0.000
Year * Season	9	1.121	0.089	12.555	0.000
Year * Prec. Y N	1	0.433	0.162	2.675	0.007
Year * Prec. Y N	2	0.714	0.163	4.386	0.000
Year * Prec. Y N	3	-0.081	0.167	-0.487	0.626
Year * Prec. Y N	4	0.368	0.173	2.127	0.033
Year * Prec. Y N	5	-0.136	0.161	-0.843	0.399
Year * Prec. Y N	6	0.132	0.137	0.964	0.335
Year * Prec. Y N	7	1.426	0.161	8.880	0.000
Year * Prec. Y N	8	-1.756	0.112	-15.736	0.000
Year * Prec. Y N	9	-0.045	0.140	-0.319	0.750
Season * Prec. Y N	1	0.624	0.050	12.487	0.000

The results of the GRM analysis, performed herein, correspond with previous, abundant research, pointing that visibility degradation is due to particulate matter, as well as relative humidity, that can greatly enhance degradation in the presence of hygroscopic aerosols [6,17,53].

#### 4. Conclusions

In Warsaw, the changes in the visibility exhibited a seasonal character. The visibility increased in summer and decreased in late autumn and winter. Mean seasonal visibilities were 24.5, 30.1, 20.1, and 13.9 km in spring, summer, autumn, and winter, respectively. The mean yearly visibility values were in the range of 19.8–23.7 km.

When the meteorological conditions were unfavourable for dispersion and transportation, the visibility was adversely affected by high pollutant concentrations ( $\text{PM}_{10}$ —236.1  $\mu\text{g}\cdot\text{m}^{-3}$ ;  $\text{SO}_2$ —28.1  $\mu\text{g}\cdot\text{m}^{-3}$ ;  $\text{CO}$ —2342.4  $\mu\text{g}\cdot\text{m}^{-3}$ ; and  $\text{NO}_2$ —76  $\mu\text{g}\cdot\text{m}^{-3}$ ). Consequently, the visibility was low (6.0 km). The unfavourable meteorological conditions involved low wind speed (approx. 1.1 m/s) and low air temperature.

On clear days, air quality was found to be good. Mean pollutant concentrations were:  $\text{PM}_{10}$ —25.7  $\mu\text{g}\cdot\text{m}^{-3}$ ;  $\text{SO}_2$ —6.8  $\mu\text{g}\cdot\text{m}^{-3}$ ;  $\text{CO}$ —378.8  $\mu\text{g}\cdot\text{m}^{-3}$ ; and  $\text{NO}_2$ —20.4  $\mu\text{g}\cdot\text{m}^{-3}$ . Mean wind speed was 2.7 m/s. Generally, the mean visibility value was 24.3 km for the good air quality days in Warsaw.

PCA helped to find that the biggest changes in the visibility in Warsaw were observed with changes in air temperature, concentrations of  $\text{PM}_{10}$ ,  $\text{CO}$ ,  $\text{NO}_2$  and  $\text{O}_3$ , and insolation. Generally, in the cold season, a fall in temperature corresponded to air pollution increase and visibility deterioration. An underlying cause for such a situation is the increase of emissions, related with fuel combustion for heating purposes.

There might also be an indirect correlation between the visibility and traffic emission in the warm (non-heating) season in Warsaw. Traffic emission influence on air quality in the warm season manifested itself with the increasing  $\text{NO}_2$  concentrations in the air without simultaneous increase of other pollutants' concentration. At the same time, there existed a decrease in concentrations of ozone, reacting photochemically under strong insolation. In such conditions the visibility increased.

Those conclusions correspond well with the GRM analyses, which demonstrated that the visibility in Warsaw was clearly affected by the measurement season and the factors-variables containing combinations of variables constructed from different measurement periods (e.g., season \* month).

It was unequivocally proven that the  $\text{PM}_{10}$  concentration was the most important parameter affecting the visibility in Warsaw. The GRM results demonstrated that the reduction in the  $\text{PM}_{10}$  concentrations by 50% (with all the remaining parameters unchanged) contributed to the increase in the visibility by 2.9 km.

#### Acknowledgments

The work was carried out within the project No 2012/07/D/ST10/02895 (ID 202319) financed by the National Science Centre Poland (NCN).

This research was supported by The Faculty of Civil and Environmental Engineering basic (statutory) research projects.

## Author Contributions

Conceived and designed the experiments: (GM).

All authors (GM, WR-K, PC, AB, AB) contributed to the data analysis and manuscript writing.

## Conflicts of Interest

The authors declare that there is no conflict of interests regarding the publication of this paper.

## References

1. Deng, J.; Xing, Z.; Zhuang, B.; Du, K. Comparative study on long-term visibility trend and its affecting factors on both sides of the Taiwan Strait. *Atmos. Res.* **2014**, *143*, 266–278.
2. Huang, W.; Tan, J.; Kan, H.; Zhao, N.; Song, W.; Song, G.; Chen, G.; Jiang, L.; Jiang, C.; Chen, R.; *et al.* Visibility, air quality and daily mortality in Shanghai, China. *Sci. Total Environ.* **2009**, *407*, 3295–3300.
3. Thach, T.Q.; Wong, C.M.; Chan, K.P.; Chau, Y.K.; Chung, Y.N.; Ou, C.Q.; Yang, L.; Hedley, A.J. Daily visibility and mortality: Assessment of health benefits from improved visibility in Hong Kong. *Environ. Res.* **2010**, *110*, 617–623.
4. Latha, K.M.; Badarinath, K.V.S. Black carbon aerosols over tropical urban environment—A case study. *Atmos. Res.* **2003**, *69*, 125–133.
5. Lee, J.Y.; Jo, W.K.; Chun, H.H. Long-Term Trends in Visibility and Its Relationship with Mortality, Air-Quality Index, and Meteorological Factors in Selected Areas of Korea. *Aerosol Air Qual. Res.* **2015**, doi:10.4209/aaqr.2014.02.0036.
6. Tsai, Y.I.; Kuo, S.C.; Lee, W.; Chen, C.L.; Chen, P.T. Long-term visibility trends in one highly urbanized, one highly industrialized, and two rural areas of Taiwan. *Sci. Total Environ.* **2007**, *382*, 324–341.
7. Deng, X.; Tie, X.; Wu, D.; Zhou, X.; Bi, X.; Tan, H.; Li, F.; Jiang, C. Long-term trend of visibility and its characterizations in the Pearl River Delta (PRD) Region, China. *Atmos. Environ.* **2008**, *42*, 1424–1435.
8. Pusheng, Z.; Zhang, X.; Xu, X.; Zhao, X. Long-Term Visibility trends and characteristics in the region of Beijing, Tianjin, and Hebei, China. *Atmos. Res.* **2011**, *101*, 711–718.
9. Fajardo, O.A.; Jiang, J.; Hao, J. Assessing young people's preferences in urban visibility in Beijing. *Aerosol Air Qual. Res.* **2013**, *13*, 1536–1543.
10. Zhuang, X.; Wang, Y.; Zhu, Z.; Querol, X.; Alastuey, A.; Rodríguez, S.; Wei, H.; Xu, S.; Lu, W.; Viana, M.; *et al.* Origin of PM10 pollution episodes in an industrialized mega-city in central China. *Aerosol Air Qual. Res.* **2014**, *14*, 338–346.
11. Rogula-Kozłowska, W.; Klejnowski, K.; Rogula-Kopiec, P.; Ośródk, L.; Krajny, E.; Błaszczak, B.; Mathews, B. Spatial and seasonal variability of the mass concentration and chemical composition of PM2.5 in Poland. *Air Qual. Atmos. Health* **2014**, *7*, 41–58.
12. Lee, C.G.; Yuan, C.S.; Chang, J.C.; Yuan, C. Effects of aerosol species on atmospheric visibility in Kaohsiung city, Taiwan. *J. Air Waste Manag. Assoc.* **2005**, *55*, 1031–1041.

13. Jung, J.; Lee, H.; Kim, Y.J.; Liu, X.; Zhang, Y.; Gu, J.; Fan, S. Aerosol chemistry and the effect of aerosol water content on visibility impairment and radiative forcing in Guangzhou during the 2006 Pearl River Delta campaign. *J. Environ. Manag.* **2009**, *90*, 3231–3244.
14. Appel, B.R.; Tokiwa, Y.; Hsu, J.; Kothny, E.L.; Hahn, E. Visibility as related to atmospheric aerosol constituents. *Atmos. Environ. (1967)* **1985**, *19*, 1525–1534.
15. Malm, W.C.; Day, D.E. Estimates of aerosol species scattering characteristics as a function of relative humidity. *Atmos. Environ.* **2001**, *35*, 2845–2860.
16. Tsai, Y.I.; Lin, Y.H.; Lee, S.Z. Visibility variation with air qualities in the metropolitan area in Southern Taiwan. *Water Air Soil Pollut.* **2003**, *144*, 19–40.
17. Tsai, Y.I. Atmospheric visibility trends in an urban area in Taiwan 1961–2003. *Atmos. Environ.* **2005**, *39*, 5555–5567.
18. Wen, C.C.; Yeh, H.H. Comparative influences of airborne pollutants and meteorological parameters on atmospheric visibility and turbidity. *Atmos. Res.* **2010**, *96*, 496–509.
19. Deng, J.; Wang, T.; Jiang, Z.; Xie, M.; Zhang, R.; Huang, X.; Zhu, J. Characterization of visibility and its affecting factors over Nanjing, China. *Atmos. Res.* **2011**, *101*, 681–691.
20. Du, K.; Mu, C.; Deng, J.; Yuan, F. Study on atmospheric visibility variations and the impacts of meteorological parameters using high temporal resolution data: An application of Environmental Internet of Things in China. *Int. J. Sustain. Dev. World Ecol.* **2013**, *20*, 238–247.
21. Majewski, G.; Czechowski, P.O.; Badyda, A.; Brandyk, A. Effect of air pollution on visibility in urban conditions. Warsaw Case Study. *Environ. Prot. Eng.* **2014**, *40*, 47–64.
22. Chen, J.; Qiu, S.; Shang, J.; Wilfrid, O.M.F.; Liu, X.; Tian, H.; Boman, J. Impact of relative humidity and water soluble constituents of PM<sub>2.5</sub> on visibility impairment in Beijing, China. *Aerosol Air Qual. Res.* **2014**, *14*, 260–268.
23. Badyda, A.; Dąbrowiecki, P.; Lubiński, W.; Czechowski, P.O.; Majewski, G.; Chciałowski, A.; Kraszewski, A. Influence of traffic-related air pollutants on lung function. *Adv. Exp. Med. Biol.* **2013**, *788*, 229–235.
24. Badyda, J.; Dąbrowiecki, P.; Czechowski, P.O.; Majewski, G.; Doboszyńska, A. Traffic-Related Air Pollution and Respiratory Tract Efficiency. *Adv. Exp. Med. Biol.* **2015**, doi:10.1007/5584\_2014\_13.
25. Majewski, G.; Kleniewska, M.; Przewoźniczuk, W. The effect of urban conurbation on the modification of human thermal perception, as illustrated by the example of Warsaw (Poland). *Theor. Appl. Climatol.* **2014**, *116*, 147–154.
26. Pastuszka, J.S.; Wawroś, A.; Talik, E.; Paw U, K.T. Optical and chemical characteristics of the atmospheric aerosol in four towns in southern Poland. *Sci. Total Environ.* **2003**, *309*, 237–251.
27. Czarnecka, M.; Nidzgorska-Lencewicz, L. Impact of weather conditions on winter and summer air quality. *Int. Agrophysics* **2011**, *25*, 7–12.
28. Rogula-Kozłowska, W.; Kozielska, B.; Błaszczak, B.; Klejnowski, K. The mass distribution of particle-bound PAH among aerosol fractions: A case-study of an urban area in Poland. In *Organic Pollutants Ten Years after the Stockholm Convention—Environmental and Analytical Update*; Puzyn, T., Mostrag-Szlichtyng, A., Eds.; InTech: Rijeka, Croatia, 2012; pp. 163–190.
29. Majewski, G.; Kleniewska, M.; Brandyk, A. Seasonal variation of particulate matter mass concentration and content of metals. *Pol. J. Environ. Stud.* **2011**, *20*, 417–427.

30. Rozbicka, K.; Majewski, G.; Rozbicki, T. Seasonal variation of air pollution in Warsaw conurbation. *Meteorol. Z.* **2014**, *23*, 175–179.
31. Majewski, G.; Rogula-Kozłowska, W. The elemental composition and origin of fine ambient particles in the largest Polish conurbation: First results from the short-term winter campaign. *Theor. Appl. Climatol.* **2015**, doi:10.1007/s00704-015-1494-y.
32. Rogula-Kozłowska, W.; Klejnowski, K.; Rogula-Kopiec, P.; Mathews, B.; Szopa, S. A study on the seasonal mass closure of ambient fine and coarse dusts in Zabrze, Poland. *Bull. Environ. Contam. Toxicol.* **2012**, *88*, 722–729.
33. Rogula-Kozłowska, W.; Rogula-Kupiec, P.; Mathews, B.; Klejnowski, K. Effects of road traffic on the ambient concentrations of three PM fractions and their main components in a large Upper Silesian city. *Ann. Wars. Univ. Life Sci.* **2013**, *45*, 243–253.
34. Rogula-Kozłowska, W. Traffic-Generated Changes in the Chemical Characteristics of Size-Segregated Urban Aerosols. *Bull. Environ. Contam. Toxicol.* **2014**, *93*, 493–502.
35. Harrison, R.M.; Deacon, A.R.; Jones, M.R. Sources and processes affecting concentrations of PM<sub>10</sub> and PM<sub>2.5</sub> particulate matter in Birmingham (UK). *Atmos. Environ.* **1997**, *31*, 4103–4117.
36. Statheropoulos, M.; Vassiliadis, N.; Pappa, A. Principal component and canonical correlation analysis for examining air pollution and meteorological data. *Atmos. Environ.* **1998**, *32*, 1087–1095.
37. Kleinbaum, D.G.; Kupper, L.L.; Muller, K.E.; Nizam, A. *Applied Regression Analysis and Other Multivariable Methods*; Duxbury Press: Pacific Grove, CA, USA, 1998; p. 798.
38. Izenman, A.J. *Modern Multivariate Statistical Techniques: Regression, Classification, and Manifold Learning*; Springer Texts in Statistics: New York, NY, USA, 2008.
39. Rozbicka, K.; Rozbicki, T. Spatiotemporal variations of tropospheric ozone concentrations in the Warsaw Agglomeration (Poland). *Ann. Wars. Univ. Life Sci.* **2014**, *46*, 247–261.
40. Xue, D.; Li, C.; Liu, Q. Visibility characteristics and the impacts of air pollutants and meteorological conditions over Shanghai, China. *Environ. Monit. Assess.* **2015**, *187*, 363, doi:10.1007/s10661-015-4581-8.
41. Cao, J.J.; Wang, Q.Y.; Chow, J.C.; Watson, J.G.; Tie, X.X.; Shen, Z.X.; Wang, P.; An, Z.S. Impacts of aerosol compositions on visibility impairment in Xi'an, China. *Atmos. Environ.* **2012**, *59*, 559–566.
42. Rogula-Kozłowska, W.; Błaszczak, B.; Kozielska, B.; Klejnowski, K. *The Mass Distribution of Particle-Bound PAH among Aerosol Fractions: A Case-Study of an Urban Area in Poland*; InTECH Open Access Publisher: Rijeka, Croatia, 2012.
43. Houthuijs, D.; Breugelmans, O.; Hoek, G.; Vaskövi, É.; Miháliková, E.; Pastuszka, J.S.; Jirik, V.; Sachelarescu, S.; Lolova, D.; Meliefste, K.; *et al.* PM<sub>10</sub> and PM<sub>2.5</sub> concentrations in Central and Eastern Europe: Results from the Cesar study. *Atmos. Environ.* **2001**, *35*, 2757–2771.
44. Pastuszka, J.S.; Okada, K. Features of atmospheric aerosol particles in Katowice, Poland. *Sci. Total Environ.* **1995**, *175*, 179–188.
45. Reizer, M.; Juda-Rezler, K. Explaining the high PM<sub>10</sub> concentrations observed in Polish urban areas. *Air Qual. Atmos. Health* **2015**, doi:10.1007/s11869-015-0358-z.
46. Pastuszka, J.S.; Rogula-Kozłowska, W.; Zajusz-Zubek, E. Characterization of PM<sub>10</sub> and PM<sub>2.5</sub> and associated heavy metals at the crossroads and urban background site in Zabrze, Upper Silesia, Poland, during the smog episodes. *Environ. Monit. Assess.* **2010**, *168*, 613–627.

47. Cleveland, W.S.; Graedel, T.E.; Kleiner, B.; Warner, J.L. Sunday and workday variations in photochemical air pollutants in New Jersey and New York. *Science* **1974**, *186*, 1037–1038.
48. Qin, Y.; Tonnesen, G.S.; Wang, Z. Weekend/weekday differences of ozone, NO<sub>x</sub>, Co, VOCs, PM<sub>10</sub> and the light scatter during ozone season in southern California. *Atmos. Environ.* **2004**, *38*, 3069–3087.
49. Marr, L.C.; Harley, R.A. Spectral analysis of weekday-weekend differences in ambient ozone, nitrogen oxide, and non-methane hydrocarbon time series in California. *Atmos. Environ.* **2002**, *36*, 2327–2335.
50. Stull, R.B. *Meteorology for Scientists and Engineers*; Brooks/Cole: Pacific Grove, CA, USA, 2000.
51. Elias, T.; Haeffelin, M.; Drobinski, P.; Gomes, L.; Rangognio, J.; Bergot, T.; Chazette, P.; Raut, J.C.; Colomb M. Particulate contribution to extinction of visible radiation: Pollution, haze, and fog. *Atmos. Res.* **2009**, *92*, 443–454.
52. Geertsema, G.T.; Schreur, B.G.J. The effect of improved nowcasting of precipitation on air quality modeling. *Atmos. Environ.* **2009**, *43*, 4924–4934.
53. Pitchford, M.; Malm, W.; Schichtel, B.; Kumar, N.; Lowenthal, D.; Hand, J. Revised algorithm for estimating light extinction from IMPROVE particle speciation data. *J. Air Waste Manag.* **2007**, *57*, 1326–1336.

© 2015 by the authors; licensee MDPI, Basel, Switzerland. This article is an open access article distributed under the terms and conditions of the Creative Commons Attribution license (<http://creativecommons.org/licenses/by/4.0/>).